JOC The Journal of Organic Chemistry

Article

pubs.acs.org/joc

Synthesis and Fluorescence Properties of Pyrimidine Mono- and Bisboron Complexes

Yasuhiro Kubota,* Yousuke Ozaki, Kazumasa Funabiki, and Masaki Matsui*

Department of Chemistry and Biomolecular Science, Faculty of Engineering, Gifu University, 1-1 Yanagido, Gifu 501-1193, Japan

Supporting Information

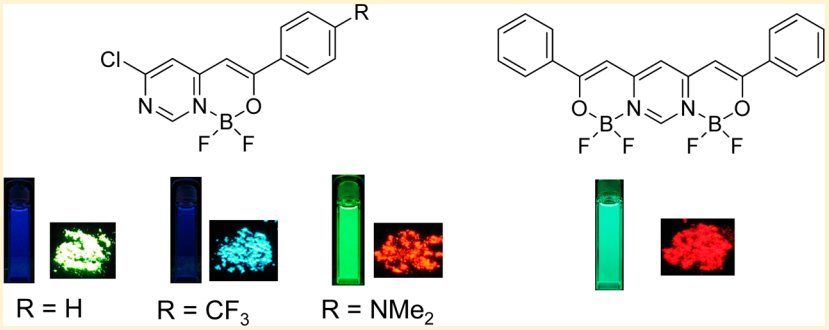

ABSTRACT: Novel fluorescent mono- and bisboron complexes based on pyrimidine bearing β-iminoenolate ligands were synthesized, and their fluorescence properties were investigated. The nonsubstituted and trifluoromethyl-substituted monoboron complexes showed higher fluorescence quantum yield in solid state than in solution. The dimethylamino derivative of the monoboron complex exhibited positive solvatochromism in the fluorescence spectra. The bisboron complex showed significantly higher molar absorption coefficient and red-shifted maximum absorption and maximum fluorescence wavelengths than the corresponding monoboron complex.

INTRODUCTION

Boron complexation is a simple yet effective strategy to express or enhance fluorescence. For example, although dipyrromethene,[1] pyridomethene,[2] diketone,[3] iminoketone,[4] and azo dyes[5] generally show no fluorescence, their boron complexes are known to be fluorescent. The boron complexes, especially boron dipyrromethene (BODIPY) dyes, show excellent fluorescence in solution and are used as molecular probes,[6] in photodynamic therapy,[7] as laser dyes[8] and solar cells.[9] However, most BODIPY dyes show small Stokes shift and lose their fluorescence in solid state.[10] Therefore, the modification of BODIPY core[11] and the development of new boron complexes[12] are being actively investigated.

On the other hand, in recent years, much attention has been paid to multinuclear boron complexes.[13] Bisboron complexes with interesting properties such as long-wavelength absorption and fluorescence,[14] fluorescent near-infrared (NIR)-labeling,[15] in vivo imaging,[16] two-photon absorption,[17] nonlinear optical properties,[18] and solid-state fluorescence[19] have been reported. Recently, we have reported that monoboron complexes based on pyrazine or thiazole structures bearing a β-iminoenolate ligand show interesting fluorescence properties such as a large Stokes shift, solid-state fluorescence and aggregation-induced emission enhancement (AIEE) effect.[4] In the course of our studies on the development of fluorescent boron complexes bearing β-iminoenolate ligands, we are interested in the synthesis of the boron complex based on pyrimidine structure. In this paper, we describe the synthesis and fluorescence properties of novel mono- and bisboron complexes based on pyrimidines bearing β-iminoenolate ligands.

RESULTS AND DISCUSSION

Synthesis. The reaction of 4,6-dichloropyrimidine with acetophenone in the presence of sodium hydride gave bidentate ligand **1**, which consists of a tautomeric mixture of iminoketone **1a** and iminoenol **1b** in $CDCl_3$ (Scheme 1). The iminoketone and iminoenol structures were confirmed by ^1H NMR spectra of the methylene signal at δ 4.47 (s, 2H) of **1a** and olefinic signal at δ 6.01 (s, 1H) and hydroxy signal at δ 14.6 (brs, 1H) of **1b**. The ratio of **1a** and **1b** was 1:15 in $CDCl_3$. The tautomeric mixture of **1** was treated with boron trifluoride diethyl ether complex in the presence of triethylamine to give monoboron complex **4**. Solution of **4** and acetophenone in tetrahydrofuran was refluxed, quenched with water, extracted with dichloromethane, and concentrated. The residue was reacted with boron trifluoride diethyl ether complex in the presence of triethylamine to yield bisboron complex **7**.

Similar reactions of 4,6-dichloropyrimidine with 4′-(trifluoromethyl)acetophenone and 4′-dimethylaminoacetophenone gave the corresponding bidentate ligands **2** and **3** (Scheme 1). The ligands **2** and **3** were allowed to react with boron trifluoride diethyl ether complex in the presence of

Received: April 25, 2013
Published: June 24, 2013

   dx.doi.org/10.1021/jo400879g | J. Org. Chem. 2013, 78, 7058−7067

Scheme 1. Synthesis of Pyrimidine Boron Complexes

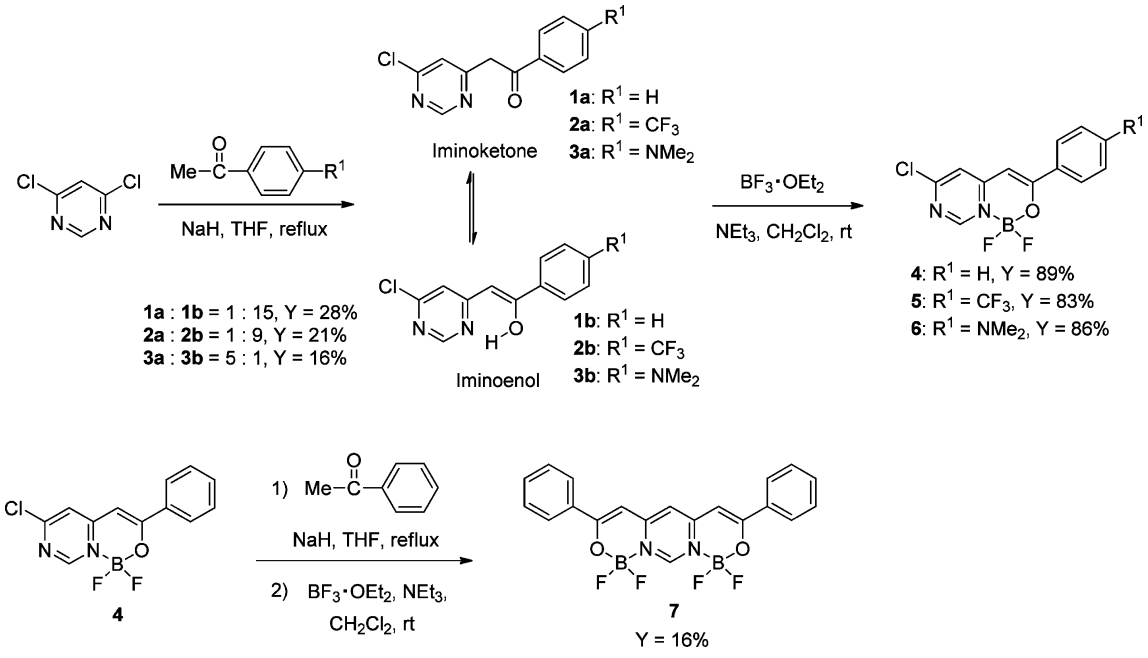

triethylamine to give trifluoromethyl- and dimethylamino-substituted BF_2 complexes **5** and **6**, respectively.

Crystal Structures. The structures of **4**–**7** were confirmed by X-ray crystallographic analysis. The ORTEP drawings of **4**–**7** are shown in Figures 1–4, respectively. The crystal structure

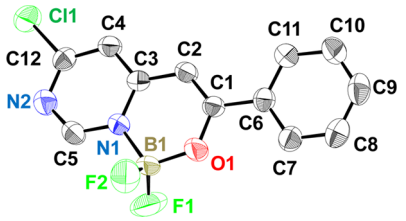

Figure 1. ORTEP view of **4** (CCDC 931994). Hydrogen atoms have been omitted for clarity.

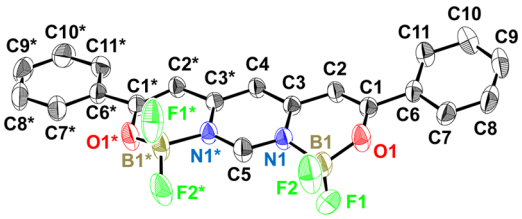

Figure 2. ORTEP view of **7** (CCDC 931992). Hydrogen atoms have been omitted for clarity.

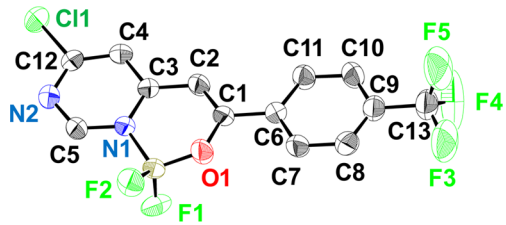

Figure 3. ORTEP view of **5** (CCDC 931993). Hydrogen atoms have been omitted for clarity.

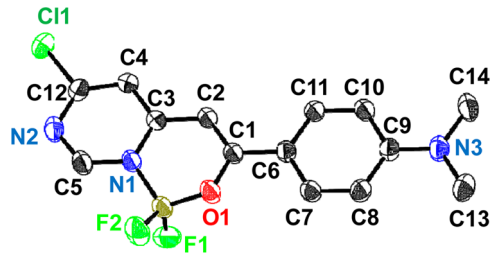

Figure 4. ORTEP view of **6** (CCDC 931995). Hydrogen atoms have been omitted for clarity.

of **7** shows C_2 symmetry along the C4–C5 axis. The C1–O1 bond lengths of **4** (1.32 Å) and **7** (1.33 Å) are between typical C–O (ca. 1.43 Å) and C=O (ca. 1.23 Å) bond lengths (Figures S1 and S2, Supporting Information). The C2–C3 (**4**: 1.41 Å, **7**: 1.42 Å) bonds are longer than C1–C2 bonds (**4**: 1.35 Å, **7**: 1.36 Å). The B1–O1 bond lengths of **4** (1.44 Å) and **7** (1.44 Å) are considerably smaller than the B1–N1 bond lengths of **4** (1.59 Å) and **7** (1.59 Å). These results suggest that the six-membered rings of **4** and **7** have delocalized iminoenolate structures.

The boron atoms of **4** and **7** have a tetrahedral geometry. Although the B1 atom of **4** lies in the same plane as the pyrimidine ring, the B1* and B1 atoms of **7** are located above and below the corresponding pyrimidine ring (Figures S1 and S2, Supporting Information). As a result, while **4** is almost planar, **7** is slightly bent. Additionally, the F2 and F1 atoms of **4** are evenly situated above and below the pyrimidine ring. On the other hand, two fluorine atoms of **7** (F1* and F1) are oriented perpendicularly above and below the pyrimidine ring, and the others (F2* and F2) are arranged horizontally to the pyrimidine ring. Furthermore, the central pyrimidine ring of **7** is more distorted than that of **4**. In the pyrimidine ring of **4**, dihedral angle between the C12–C4–C3 plane and the N2–C5–N1 plane is 0.5° (Figure S1, Supporting Information). Meanwhile, in the case of **7**, the corresponding dihedral angle is 2.2° (Figure S2, Supporting Information). The adjacent

dx.doi.org/10.1021/jo400879g | J. Org. Chem. 2013, 78, 7058–7067

bidentate coordination of two boron atoms through the pyrimidine moiety causes a larger distortion in the structure of **7** than in that of **4**. This may be due to the relief of the steric repulsion between neighboring boron moieties.

The torsion angles of C2−C1−C6−C7 of **4**−**7** are 5.9°, 0.8°, 6.7° and 10.2°, respectively (Figure S3, Supporting Information). This indicates that the terminal aryl groups allow the extension of π-conjugation. The C1−C6 bond length of **4**−**7** is as follows: 1.477 Å for **4**, 1.481 Å for **5**, 1.461 Å for **6** and 1.479 Å for **7** (Figure S3, Supporting Information). The C1−C6 bond length of **6** is shorter than those of **4**, **5** and **7**, suggesting that contribution of the resonance structure shown in Figure S4 (Supporting Information) is important in the ground state of **6**.

Optical Properties. The UV−vis absorption and normalized fluorescence spectra of **4**−**7** in dichloromethane are shown in Figures 5 and 6, respectively. The maximum absorption wavelength (λ_{max}) of monoboron complex **4** (375 nm) was slightly red-shifted compared to that of ligand **1** (346 nm) (Table 1). Although ligand **1** did not show fluorescence, complex **4** exhibited weak blue fluorescence at 429 nm. The fluorescence quantum yields (Φ_f) of **1** and **4** in dichloromethane were 0.00 and 0.02, respectively. Bisboron complex **7** showed a sharp absorption peak at 475 nm along with a vibrational peak at 449 nm. The λ_{max} of **7** was 100 nm red-shifted compared to that of **4**. Molar absorption coefficient (ε) of **7** (107,300) was significantly higher than that of **4** (42,600), which may be because of the extension of π-conjugation by annulation and the two terminal phenyl groups. Bisboron complex **7** exhibited relatively strong yellow-green fluorescence (Φ_f = 0.55), and the maximum fluorescence wavelength (F_{max}) was 490 nm. The Stokes shift of **7** (645 cm^{-1}) was very small, similar to other boron complexes such as BODIPY dyes[1] (400−600 cm^{-1}, in most cases) and pyridomethene−BF_2 complexes[2b] (250−400 cm^{-1}). This suggests that **7** has rigid molecular structure with little difference between the ground and excited-state structures.[20] The λ_{max} of **5** (372 nm) was slightly blue-shifted, and ε was lower (35,800) compared to that of **4** (375 nm and 42,600), respectively. On the other hand, **6** showed relatively large bathochromic shift of λ_{max} (459 nm) and increase in ε (70,800).

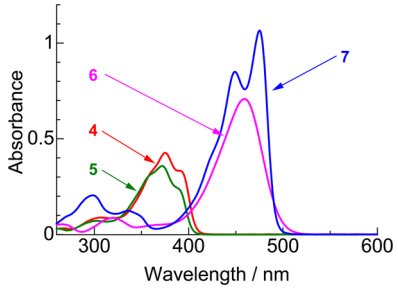

Figure 5. UV−vis absorption spectra of **4**−**7** in dichloromethane (1.0×10^{-5} M).

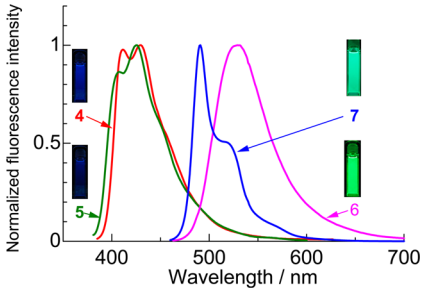

Figure 6. Normalized fluorescence spectra of **4**−**7** in dichloromethane (1.0×10^{-5} M).

Theoretical Calculation. To understand the absorption properties of **4**−**7**, density functional theory (DFT) calculations were performed with a Gaussian 09 package.[21] The geometries were optimized at DFT/B3LYP level using a 6-31G(d,p) basis set. Time-dependent DFT (TDDFT) calculations were also performed using a B3LYP/6-311++G(d,p) method. The calculated λ_{max}, main orbital transition, and oscillator strength f are listed in Table S1 (Supporting Information). For all complexes, the first absorptions are mostly attributed to HOMO−LUMO transitions. For each complex, the HOMO and LUMO orbitals are delocalized over the whole molecule (Figure 7). In particular, in the case of **7**, the two terminal phenyl rings significantly contribute to the delocalization. Therefore, bisboron complex **7** is expected to have red-shifted λ_{max} and high ε. The DFT calculations indicate that dimethylamino derivative **6** shows intramolecular charge-transfer (ICT) transition from dimethylamino group to the pyrimidine moiety. The red-shifted λ_{max} of **6** are owing to the ICT transition.

Discussion of Fluorescence Quantum Yield in Solution. Although complexes **4** and **5** hardly showed any fluorescence ($\Phi_f \leq 0.02$), complexes **6** (Φ_f = 0.78) and **7** (Φ_f = 0.55) exhibited relatively strong fluorescence. Recently, we reported that thiazole−monoboron complexes bearing β-

Table 1. Optical Properties of Pyrimidine Boron Complexes

	in dichloromethane[a]						solid state	
compd	λ_{max} [nm] (ε)	F_{max}[b] [nm]	Φ_f[b,c]	τ_s[d] [ns]	k_f[e] [10^9 s^{-1}]	k_{nr}[f] [10^9 s^{-1}]	F_{max}[g] [nm]	Φ_f[c,g]
4	375 (42,600)	411, 429	0.02	—[h]	—	—	525	0.13
	391 (33,300)							
5	372 (35,800)	407, 426	0.01	—[h]	—	—	488	0.15
	388 (24,000)							
6	459 (70,800)	529	0.78	2.8	0.28	0.08	629	0.20
7	449 (85,000)	490, 517	0.55	1.4	0.39	0.32	641	0.07
	475 (107,300)							

[a]Measured at a concentration of 1.0×10^{-5} mol dm^{-3}. [b]The excitation wavelengths (λ_{ex}) were as follows: **4** (377 nm), **5** (377 nm), **6** (452 nm), and **7** (464 nm). [c]Measured using an integrating sphere method. [d]Measured using a single-photon-counting method. [e]Radiative rate constant ($k_f = \Phi_f/\tau_s$). [f]Nonradiative rate constant ($k_{nr} = (1 - \Phi_f)/\tau_s$). [g]The λ_{ex} were as follows: **4** (368 nm), **5** (372 nm), **6** (523 nm), and **7** (504 nm). [h]Too short to be measured (τ_s < 0.1 ns).

dx.doi.org/10.1021/jo400879g | J. Org. Chem. 2013, 78, 7058−7067

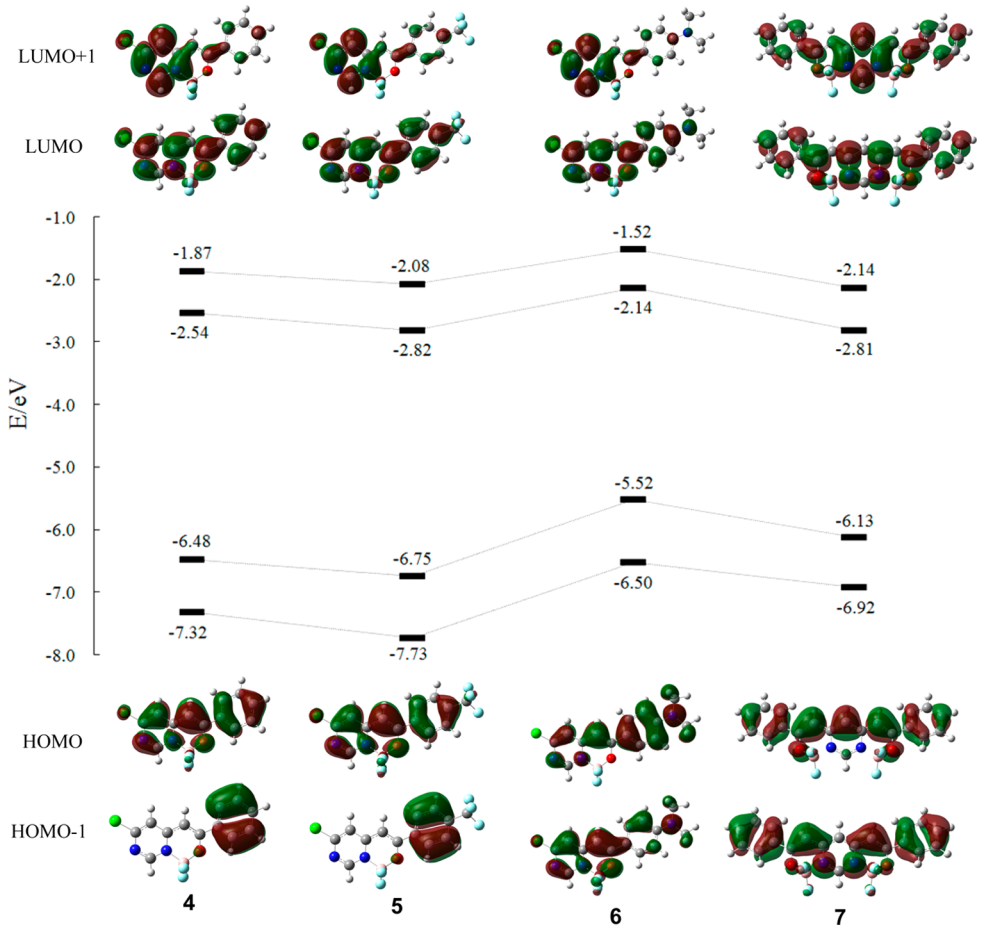

Figure 7. Molecular orbital energy diagram and isodensity surface plots of the HOMO−1, HOMO, LUMO, and LUMO+1 of **4**−**7**.

iminoenolate hardly show fluorescence in solution because of the intramolecular C−Ar rotation, which promotes nonradiative processes.[4b] In order to consider the effect of the C−Ar rotation on the Φ_f value, we investigated the fluorescence properties of **4** in THF−water mixtures of various rations. The fluorescence color and F_{max} were almost unchanged until the addition of 80% water by volume, because **4** was soluble in the THF−water mixtures. However, when the water fraction exceeded 85%, the fluorescence color and F_{max} were dramatically changed from blue to yellow-green and from 430 to 520 nm, respectively (Figures S5 and S6, Supporting Information). The fluorescence intensity was also increased with increasing the water fraction. As described below in detail, **4** has higher Φ_f value and more red-shifted F_{max} in solid state than in solution. Thus, these changes are considered to result from the formation of aggregates in the THF−water mixtures: the formation of nanoparticles was confirmed by the observation of the Tyndall phenomenon (Figure S7, Supporting Information). Since molecular rotations are restricted in the solid state, the observed increase of fluorescence intensity indicates the intramolecular C−Ar rotation causes the fluorescence quenching in solution.[4b,22] However, in the light of the fact that the nonradiative rate constant (k_{nr}) of **7** (0.32×10^9 s^{-1}) having two phenyl groups is small compared to those of **4** (5.00×10^9 s^{-1}) and **5** (4.57×10^9 s^{-1}), there may be other process in the nonradiative decay of **4** such as a heavy-atom effect of chlorine (Tables S2 and S3, Supporting Information).[23]

The k_{nr} value of **6** (0.08×10^9 s^{-1}) was obviously smaller than those of **4** and **5**. This suggests that the higher Φ_f value of **6** is due to the suppression of nonradiative processes. In the case of **6**, the resonance structure predicts the restriction of the C−Ar rotation (Figure S4, Supporting Information). Therefore, the higher Φ_f value of **6** may be because of not only the difference of the transition between **4**, **5** (π−π^* transition) and **6** (ICT transition), but also the restriction of the intramolecular C−Ar rotation.

Solvent Effect. The effects of solvent on the absorption and fluorescence properties of **4**−**6** were investigated. The λ_{max}, ε and F_{max} values of **4** and **5** were slightly affected by the type of solvent (Figures S8−S11, Tables S2 and S3, Supporting Information). Moreover, the absorption spectra of **6** were hardly affected by the solvent (Figure 8). However, **6** showed pronounced positive solvatochromism in the fluorescence spectra (Figures 9 and Table 2). As the solvent polarity increased, the fluorescence spectra got red-shifted and broadened. To estimate the difference in dipole moments between the excited state and ground state ($\Delta\mu$), Lippert−Mataga plot of **6** was created (Figures 10 and 11).[24] Solvent polarity parameters (Δf) are obtained from the equation shown in Figure 10.[25] The radius of Onsager cavity was calculated by B3LYP/6-31G(d,p) method (a = 4.98 Å). The $\Delta\mu$ value of **6** was estimated to be 11.4 D from the slope of Lippert−Mataga plot (10,630 cm^{-1}). The dipole moment in the ground state (μ_g) was calculated to be 9.17 D by using B3LYP/6-31G(d,p) method. Therefore, the dipole moment of **6** in the excited state (μ_e) was estimated to be ca. 20.6 D. The high μ_e value suggests

dx.doi.org/10.1021/jo400879g | J. Org. Chem. 2013, 78, 7058−7067

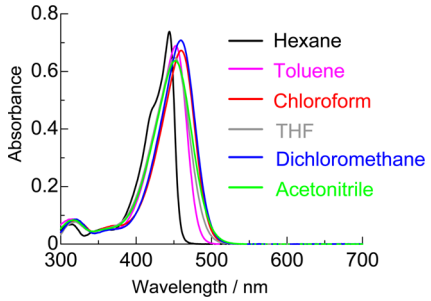

Figure 8. UV−vis absorption spectra of **6** in various solvents (1.0×10^{-5} M).

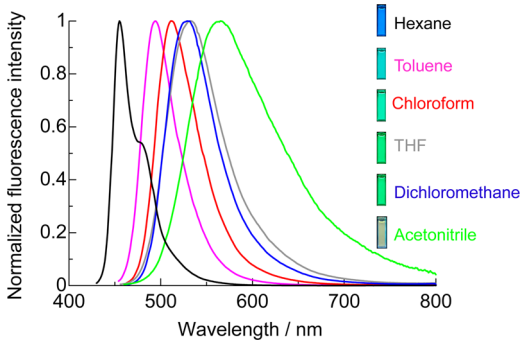

Figure 9. Normalized fluorescence spectra of **6** in various solvents (1.0×10^{-5} M).

the formation of ICT-excited state with higher dipolar moment than the ground state.[26] Because the ICT-excited state is stabilized in more polar solvents, F_{max} red-shifted with increasing solvent polarity.

Solid-State Fluorescence. Boron complexes **4**−**7** showed solid-state fluorescence (Table 1). The fluorescence spectra of **4**−**7** are shown in Figure 12. The Φ_f values were as follows: 0.13 (**4**), 0.15 (**5**), 0.20 (**6**), and 0.07 (**7**). Interestingly, monoboron complexes **4** and **5** showed higher Φ_f values in solid state than in solution ($\Phi_f \leq 0.05$); in other words, **4** and **5** have aggregation-induced enhanced emission (AIEE) character. This is probably because of the restriction of intramolecular C−Ar rotation in the solid state.[4b,22]

To consider the differences in Φ_f, we investigated the crystal packing of **4**−**7**. In the crystal packing of **7**, the molecules depicted in blue and red (Figure 13) formed independent stacking columns **7A** and **7B** by intermolecular $\pi-\pi$ interactions (C−C: 3.40−3.67 Å). Furthermore, $\pi-\pi$ interactions (C−C: 3.56−3.69 Å) were observed between the columns **7A** and **7B**. As a result, bisboron complex **7** formed consecutive intermolecular $\pi-\pi$ interactions throughout the molecule. In many cases, strong and continuous intermolecular interactions between the neighboring fluorophores cause fluorescence quenching in the solid state.[27] Therefore, because of the consecutive $\pi-\pi$ interactions, **7** is considered to have relatively low Φ_f (0.07).

In the case of **4**, the molecules depicted in blue and red as well as in orange and gray formed dimers by $\pi-\pi$ interactions (C−C: 3.36−3.70 Å) (Figure 14). Additionally, $\pi-\pi$ interactions were observed for each of the dimers (C−C: 3.52−3.69 Å). Thus, similar to **7**, independent stacking columns **4A** and **4B** were formed by consecutive $\pi-\pi$ interactions. However, $\pi-\pi$ interactions between the columns **4A** and **4B** were not observed. Because the interactions between the stacking columns were inhibited, monoboron complex **4** could exhibit higher Φ_f (0.13) than **7**.

As shown in Figure 15, trifluoromethyl derivative **5** also formed dimers by $\pi-\pi$ interactions (C−C: 3.58−3.70 Å). Similar to **4**, stacking columns **5A** and **5B** were formed by $\pi-\pi$ interactions between each of the dimers (C−C: 3.63 Å) in the crystal of **5**. However, the interactions between the dimers of **5** (C−C: 3.63 Å) were weaker than those of **4** (C−C: 3.52−3.69 Å). Therefore, **5** is considered to have weaker intermolecular interactions than **4**, and the slightly higher Φ_f of **5** (0.15) is probably owing to the weak $\pi-\pi$ interactions.

In the crystal packing of **6**, dimers were formed by $\pi-\pi$ interactions between the molecules presented in blue and red (C−C: 3.47−3.68 Å) (Figure 16). However, unlike the other boron complexes, there were no $\pi-\pi$ interactions between the adjacent dimers. Because of the inhibition of interactions between the dimers, **6** exhibited relatively strong Φ_f (0.20) compared to the other complexes.

CONCLUSIONS

In conclusion, we synthesized mono- and bisboron complexes based on pyrimidine bearing β-iminoenolate ligands and investigated their fluorescence properties both in solution and in solid states. Although the nonsubstituted and trifluoromethyl-substituted monoboron complexes hardly showed any fluorescence in dichloromethane (F_{max}: 425−428 nm, Φ_f = 0.02), relatively strong fluorescence was observed in solid state (F_{max}: 488−525 nm, Φ_f: 0.13−0.15), probably because of the restriction of intramolecular C−Ar rotation that promotes the nonradiative processes. The dimethylamino-substituted monoboron complex exhibited strong and relatively red-shifted fluorescence in dichloromethane (F_{max}: 529 nm, Φ_f = 0.78). The F_{max} of the dimethylamino derivative red-shifted with increasing solvent polarity (F_{max}: 456−565 nm). The DFT

Table 2. Absorption and Fluorescence Properties of 6 in Various Solvents

solvent[a]	Δf[b]	λ_{max} [nm] (ε)	F_{max}[c] [nm]	Stokes shift [cm^{-1}]	Φ_f[c,d]	τ_s[e] [ns]	k_f[f] [10^9 s^{-1}]	k_{nr}[g] [10^9 s^{-1}]
hexane	0.00	444 (73,900)	456	593	0.82	1.9	0.44	0.10
toluene	0.02	453 (68,900)	494	1832	0.84	2.3	0.37	0.07
chloroform	0.15	460 (67,300)	512	2208	0.82	2.5	0.32	0.07
THF	0.21	451 (64,800)	532	3376	0.60	2.6	0.23	0.15
dichloromethane	0.22	459 (70,800)	529	2882	0.78	2.8	0.28	0.08
acetonitrile	0.31	452 (63,800)	565	4425	0.03	0.3	0.11	3.46

[a]Measured at a concentration of 1.0×10^{-5} mol dm^{-3}. [b]Solvent polarity parameter ($[(\varepsilon - 1)/(2\varepsilon + 1)] - [(n^2 - 1)/(2n^2 + 1)]$) (ref 25). [c]The excitation wavelengths (λ_{ex}) were as follows: hexane (445 nm), toluene (452 nm), chloroform (458 nm), THF (451 nm), dichloromethane (452 nm), and acetonitrile (451 nm). [d]Measured using an integrating sphere method. [e]Measured using a single-photon-counting method. [f]Radiative rate constant ($k_f = \Phi_f/\tau_s$). [g]Nonradiative rate constant ($k_{nr} = (1 - \Phi_f)/\tau_s$).

dx.doi.org/10.1021/jo400879g | J. Org. Chem. 2013, 78, 7058−7067

$$\Delta\upsilon = \upsilon_{abs} - \upsilon_{fl}$$
$$= \frac{1}{4\pi\varepsilon_0}\frac{2\Delta\mu^2}{hca^3}\Delta f + \text{constant}$$
$$= \frac{(9.05\times10^{34})\,\Delta\mu^2}{a^3}\Delta f\ [C^{-2}] + \text{constant}$$
$$\Delta f = \frac{\varepsilon - 1}{2\varepsilon + 1} - \frac{n^2 - 1}{2n^2 + 1}$$

$\Delta\upsilon$: Stokes shift.
υ_{abs} : Wavenumber of absorption maximum.
υ_{fl} : Wavenumber of fluorescence maximum.
ε_0 : Dielectric constant of vacuum.
$\Delta\mu$: The difference in the dipole moment between excited and ground states.
h : Planck constant.
c : Light velocity.
a : Radius of Onsager cavity.
Δf : Orientation polarizability.
ε : Dielectric constant of solvent.
n : Refractive index of solvent.

Figure 10. Lippert−Mataga equation.

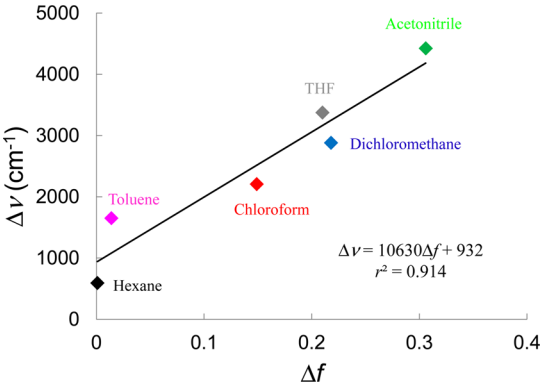

Figure 11. Lippert−Mataga plot of **6**.

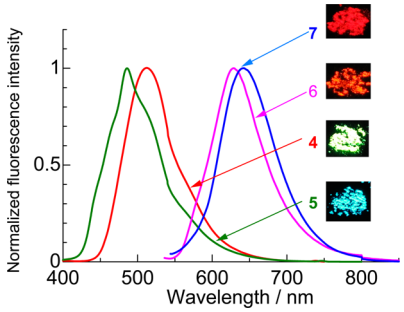

Figure 12. Normalized fluorescence spectra of **4**−**7** in the solid state.

calculation result and relatively large μ_e value (20.6 D) obtained from Lippert−Mataga plot suggest the formation of ICT-excited state. The dimethylamino derivative showed the highest Φ_f (0.20) in solid state because of the inhibition of consecutive π−π intermolecular interactions. The bisboron complex had higher ε (107,300) as well as red-shifted λ_{max} (475 nm) and F_{max} (490 nm) compared to the corresponding nonsubstituted monoboron complex, probably because of the extension of π-conjugation by annulation and the two terminal phenyl groups.

EXPERIMENTAL SECTION

General Methods. NMR spectra were recorded on 400 or 600 MHz spectrometers. Chemical shifts are referred to TMS (^{1}H and ^{13}C) as internal standards and $CFCl_3$ (^{19}F) as an external standard. Infrared (IR) spectra were recorded in KBr pallets. UV−vis and fluorescence spectra were recorded in a quartz cell (light path: 10 mm). Absolute fluorescence quantum yields were measured using an integrating sphere. Fluorescence lifetimes were measured by a single-photon-counting method. Mass spectra were measured in electron impact (EI) mode. Melting points were measured on a Yanagimoto MP−S2 micro-melting-point apparatus. Analytical thin-layer chromatography (TLC) was performed on precoated plates (Merck, silica gel 60 F254). Silica gel (Wakogel C−200) was used for column chromatography. Crystallographic X-ray data were collected using Mo Kα radiation.

Synthesis of 1. Sodium hydride (60 wt % in oil, 1.61 g, 40.3 mmol) was added to a THF (150 mL) solution of 4,6-dichloropyrimidine (2.00 g, 13.4 mmol) and acetophenone (3.22 g, 26.8 mmol) at room temperature. The solution was refluxed for 1 day. After cooling to room temperature, water was added to the reaction mixture and extracted with dichloromethane. The extract was dried over Na_2SO_4 and concentrated in vacuo. Column chromatography of the residue on silica gel (CH_2Cl_2, R_f = 0.3), followed by recrystallization from ethanol to give **1** (875 mg, 28%, **1a**:**1b** = 1:15 in $CDCl_3$) as a yellow-white powder. **1** (mixture of **1a** and **1b**): mp 112.0−104.0 °C; UV−vis (CH_2Cl_2) λ_{max} 346 nm (log ε = 4.41); IR (KBr) 3070, 1628, 1566, 1415, 1057, 1096, 864, 756 cm^{-1}; EIMS (m/z) (rel intensity) 234 ([M+2]$^+$; 8), 280 (M$^+$; 23), 105 (100). Anal. Calcd for $C_{12}H_9ClN_2O$: C, 61.95; H, 3.90; N, 12.04. Found: C, 61.98; H, 4.04; N, 11.74. **1b**: ^{1}H NMR (400 MHz, $CDCl_3$) δ 6.01 (s, 1H), 7.03 (s, 1H), 7.43−7.50 (m, 3H), 7.85 (d, J = 7.4 Hz, 2H), 8.72 (s, 1H), 14.6 (s, 1H); ^{13}C NMR (100 MHz, $CDCl_3$) δ 92.9, 116.5, 126.1, 128.6, 130.9, 134.6, 155.5, 160.3, 165.3, 169.2.

Synthesis of 2. Sodium hydride (60 wt % in oil, 1.61 g, 40.3 mmol) was added to a THF (150 mL) solution of 4,6-dichloropyrimidine (2.00 g, 13.4 mmol) and 4′-(trifluoromethyl)-acetophenone (4.45 g, 23.7 mmol) at room temperature. The solution was refluxed for 1 day. After cooling to room temperature, water was added to the reaction mixture and extracted with dichloromethane. The extract was dried over Na_2SO_4 and concentrated in vacuo. Column chromatography of the residue on silica gel (CH_2Cl_2, R_f = 0.7), followed by recrystallization from ethanol gave **2** (852 mg, 21%, **2a**:**2b** = 1:9 in $CDCl_3$) as a yellow-white powder. **2** (mixture of **2a** and **2b**): mp 101.0−103.0 °C; IR (KBr) 3086, 1632, 1574, 1424, 1335, 1115, 1072, 910 cm^{-1}; UV−vis (CH_2Cl_2) λ_{max} 344 nm (log ε = 4.60); EIMS (m/z) (rel intensity) 302 ([M+2]$^+$; 23), 300 (M$^+$; 68), 299 (73), 173 (100), 145 (67). Anal. Calcd for $C_{13}H_8ClF_3N_2O$: C, 51.93; H, 2.68; N, 9.32. Found: C, 51.67; H, 2.62; N, 9.31. **2a**: ^{1}H NMR (400 MHz, $CDCl_3$) δ 4.48 (s, 2H), 7.44 (s, 1H), 7.78 (d, J = 8.6 Hz, 2H), 8.15 (d, J = 8.6 Hz, 2H), 8.95 (s, 1H). **2b**: ^{1}H NMR (400 MHz, $CDCl_3$) δ 6.05 (s, 1H), 7.08 (s, 1H), 7.70 (d, J = 8.5 Hz, 2H), 7.94 (d, J = 8.5 Hz, 2H), 8.76 (s, 1H), 14.6 (s, 1H); ^{13}C NMR (100 MHz, $CDCl_3$) δ 94.2, 117.1, 123.9 (q, J = 274.1 Hz), 125.6, 126.5, 132.4 (q, J = 33.4 Hz), 138.1, 155.7, 160.9, 165.0, 167.2; ^{19}F NMR (376 MHz, $CDCl_3$, ext. $CFCl_3$) δ −62.7 (s, 3F).

Synthesis of 3. Sodium hydride (60 wt % in oil, 1.61 g, 40.3 mmol) was added to a THF (150 mL) solution of 4,6-dichloropyrimidine (2.00 g, 13.4 mmol) and 4′-dimethylaminoaceto-phenone (3.45 g, 21.1 mmol) at room temperature. The solution was refluxed for 2 days. After cooling to room temperature, water was added to the reaction mixture and extracted with dichloromethane. The extract was dried over Na_2SO_4 and concentrated in vacuo. Column chromatography of the residue on silica gel (CH_2Cl_2:AcOEt = 20:1, R_f = 0.4), followed by recrystallization from ethanol gave **3** (582 mg, 16%, **3a**:**3b** = 5:1 in $CDCl_3$) as a yellow-white powder. **3** (mixture

dx.doi.org/10.1021/jo400879g | J. Org. Chem. 2013, 78, 7058−7067

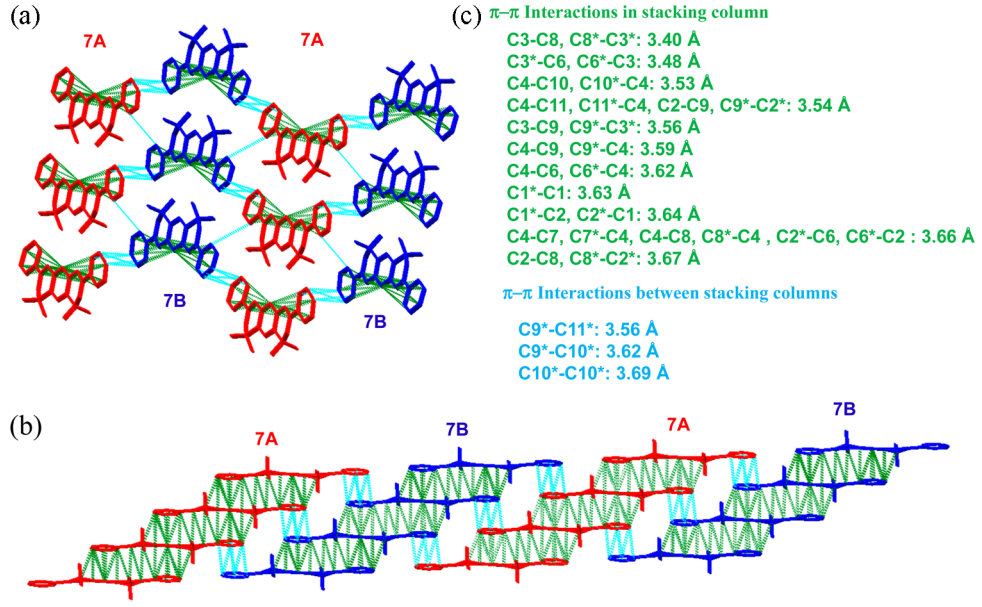

Figure 13. (a) Top view of the crystal structure of **7** ($Z = 2$). (b) Side view of the crystal structure of **7**. (c) List of intermolecular interactions of **7**. Green- and light blue-dotted lines show $\pi-\pi$ interactions in a stacking column and between the stacking columns, respectively.

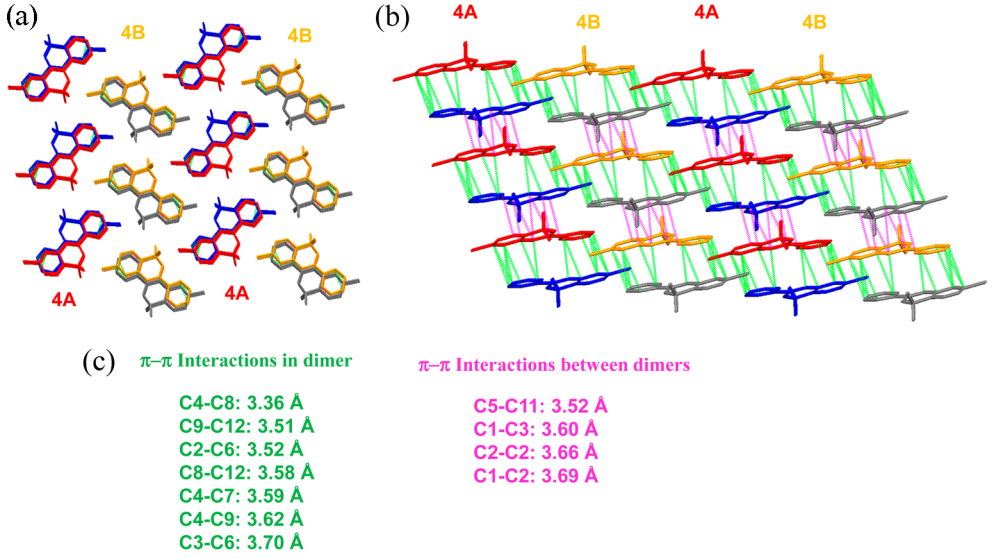

Figure 14. (a) Top view of the crystal structure of **4** ($Z = 4$). (b) Side view of the crystal structure of **4**. (c) List of intermolecular interactions of **4**. Green- and pink-dotted lines show $\pi-\pi$ interactions in a dimer and between the dimers, respectively.

of **3a** and **3b**): mp 194.0−196.0 °C; IR (KBr) 3059, 1659, 1601, 1570, 1531, 1377, 1331, 1246, 1200, 818 cm^{-1}; UV−vis (CH_2Cl_2) λ_{max} 342 nm (log ε = 4.60), 406 nm (log ε = 3.97); EIMS (m/z) (rel intensity) 277 ($[M+2]^+$; 10), 275 (M^+; 30), 148 (100). Anal. Calcd for $C_{14}H_{14}ClN_3O$: C, 60.98; H, 5.12; N, 15.24. Found: C, 61.04; H, 5.03; N, 15.03. **3a**: ^1H NMR (400 MHz, $CDCl_3$) δ 3.08 (s, 6H), 4.36 (s, 2H), 6.67 (d, J = 9.2 Hz, 2H), 7.44 (s, 1H), 7.93 (d, J = 9.2 Hz, 2H), 8.93 (s, 1H); ^{13}C NMR (150 MHz, $CDCl_3$) δ 40.0, 46.6, 110.8, 122.2, 127.7, 131.1, 153.9, 158.6, 161.3, 166.6, 192.2. **3b**: ^1H NMR (400 MHz, $CDCl_3$) δ 3.05 (s, 6H), 5.87 (s, 1H), 6.73 (d, J = 8.3 Hz, 2H), 6.91 (s, 1H), 7.76 (d, J = 8.3 Hz, 2H), 8.60 (s, 1H), 14.7 (brs, 1H); ^{13}C NMR (150 MHz, $CDCl_3$) δ 40.1, 90.0, 111.4, 115.5, 121.6, 123.8, 152.2, 155.3, 159.5, 165.4, 170.5.

Synthesis of 4. Ligand **1** (500 mg, 2.15 mmol) was dissolved in dry dichloromethane (100 mL). Triethylamine (0.74 mL, 5.3 mmol) and boron trifluoride diethyl ether complex (0.68 mL, 5.4 mmol) were added to the solution and stirred at room temperature for 6 h. Then water was added to the solution. The solution was extracted with CH_2Cl_2. The organic layer was dried over Na_2SO_4. After concentration of solvent, the residue was purified via chromatography with silica gel (CH_2Cl_2, R_f = 0.6), followed by recrystallization from chloroform to afford **4** (537 mg, 89%) as a yellow solid. **4**: mp 281.0−282.0 °C; ^1H NMR (600 MHz, $CDCl_3$) δ 6.33 (s, 1H), 7.20 (s, 1H), 7.49 (dd, J = 7.6, 7.6 Hz, 2H), 7.57 (t, J = 7.6 Hz, 1H), 7.97 (d, J = 7.6 Hz, 2H), 8.84 (s, 1H); ^{13}C NMR (100 MHz, DMSO-d_6) δ 92.9, 117.5, 127.4, 129.7, 133.1, 133.2, 152.6, 157.2, 162.0, 167.4; ^{19}F NMR (565 MHz, $CDCl_3$, ext. $CFCl_3$) δ −137.9 (q, J = 12.1 Hz, 2F); IR (KBr) 3090, 1597, 1512, 1396, 1138, 1096, 1053, 1033 cm^{-1}; EIMS (m/z) (rel intensity) 282 ($[M+2]^+$; 17), 280 (M^+; 56), 279 (100), 77 (17). Anal. Calcd for $C_{12}H_8BClF_2N_2O$: C, 51.39; H, 2.88; N, 9.99. Found: C, 51.15; H, 2.92; N, 9.97.

Synthesis of 5. Ligand **2** (500 mg, 1.66 mmol) was dissolved in dry dichloromethane (100 mL). Triethylamine (0.60 mL, 4.3 mmol) and boron trifluoride diethyl ether complex (0.55 mL, 4.4 mmol) were added to the solution and stirred at room temperature for 6 h. Then water was added to the solution. The solution was extracted with

dx.doi.org/10.1021/jo400879g | J. Org. Chem. 2013, 78, 7058−7067

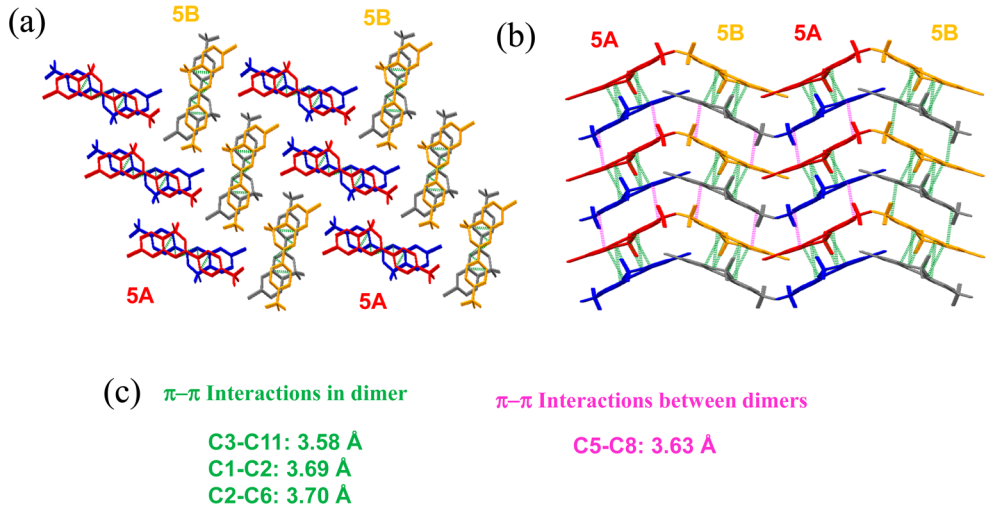

Figure 15. (a) Top view of the crystal structure of **5** ($Z = 4$). (b) Side view of the crystal structure of **5**. (c) List of intermolecular interactions of **5**. Green- and pink-dotted lines show $\pi-\pi$ interactions in a dimer and between the dimers, respectively.

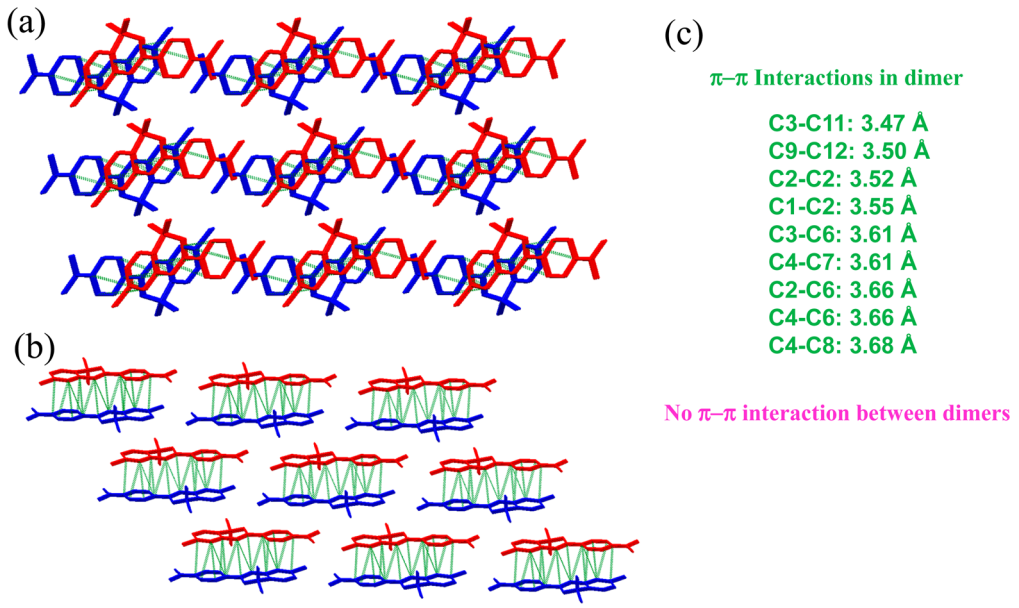

Figure 16. (a) Top view of the crystal structure of **6** ($Z = 2$). (b) Side view of the crystal structure of **6**. (c) List of intermolecular interactions of **6**. Green-dotted lines show $\pi-\pi$ interactions in a dimer.

CH_2Cl_2. The organic layer was dried over Na_2SO_4. After concentration of solvent, the residue was purified via chromatography with silica gel (CH_2Cl_2, $R_f = 0.8$), followed by recrystallization from chloroform to afford **5** (480 mg, 83%) as a yellow solid. **5**: mp 209.0–210.0 °C; ^{1}H NMR (400 MHz, $CDCl_3$) δ 6.39 (s, 1H), 7.29 (s, 1H), 7.75 (d, $J = 8.2$ Hz, 2H), 8.07 (d, $J = 8.2$ Hz, 2H), 8.91 (s, 1H); ^{13}C NMR (100 MHz, $CDCl_3$) δ 92.5, 116.2, 123.6 (q, $J = 276.5$ Hz), 125.9, 127.7, 134.1 (q, $J = 33.4$ Hz), 136.3, 151.9, 156.7, 163.4, 168.1; ^{19}F NMR (376 MHz, $CDCl_3$, ext. $CFCl_3$) δ −137.7 (q, $J = 11.9$ Hz, 2F), −63.0 (s, 3F); IR (KBr) 3093, 1601, 1508, 1327, 1130, 1069 cm^{-1}; EIMS (m/z) (rel intensity) 350 ([M+2]$^+$; 18), 348 (M$^+$; 61), 347 (100). Anal. Calcd for $C_{13}H_7BClF_5N_2O$: C, 44.81; H, 2.02; N, 8.04. Found: C, 44.76; H, 1.99; N, 7.98.

Synthesis of 6. Ligand **3** (600 mg, 2.18 mmol) was dissolved in dry dichloromethane (100 mL). Triethylamine (0.90 mL, 6.5 mmol) and boron trifluoride diethyl ether complex (0.83 mL, 6.6 mmol) were added to the solution and stirred at room temperature for 6 h. Then water was added to the solution. The solution was extracted with CH_2Cl_2. The organic layer was washed with water and dried over $MgSO_4$. After concentration of solvent, the residue was purified via chromatography with silica gel (CH_2Cl_2, $R_f = 0.4$) to afford **6** (606 mg, 86%) as a red solid. **6**: mp 273.0–275.0 °C; ^{1}H NMR (400 MHz, $CDCl_3$) δ 3.10 (s, 6H), 6.12 (s, 1H), 6.68 (d, $J = 8.9$ Hz, 2H), 7.00 (s, 1H), 7.87 (d, $J = 8.9$ Hz, 2H), 8.65 (s, 1H); ^{13}C NMR (100 MHz, $CDCl_3$) δ40.1, 88.4, 111.2, 114.6, 119.3, 127.7, 151.6, 153.5, 156.1, 160.4, 170.8; ^{19}F NMR (565 MHz, $CDCl_3$, ext. $CFCl_3$) δ −139.2 (q, $J = 13.6$ Hz, 2F); IR (KBr) 3117, 1586, 1500, 1431, 1396, 1196 cm^{-1}; EIMS (m/z) (rel intensity) 325 ([M+2]$^+$; 32), 323 (M$^+$; 100), 149 (17). Anal. Calcd for $C_{14}H_{13}BClF_2N_3O$: C, 51.97; H, 4.05; N, 12.99. Found: C, 52.23; H, 4.05; N, 12.72.

Synthesis of 7. Sodium hydride (60 wt % in oil, 172 mg, 4.29 mmol) was added to a THF (150 mL) solution of **4** (400 mg, 1.43 mmol) and acetophenone (205 mg, 1.71 mmol) at room temperature. The solution was refluxed for 2 days. After cooling to room temperature, water was added to the reaction mixture and extracted with dichloromethane. The extract was dried over Na_2SO_4 and concentrated in vacuo. The residue was dissolved in dry dichloromethane (70 mL). Triethylamine (1.0 mL, 7.2 mmol) and boron trifluoride diethyl ether complex (0.90 mL, 7.2 mmol) were added to the solution and stirred at room temperature for 6 h. Then water was

dx.doi.org/10.1021/jo400879g | J. Org. Chem. 2013, 78, 7058–7067

added to the solution. The solution was extracted with dichloromethane. The organic layer was dried over Na_2SO_4. After concentration of solvent, the residue was purified via chromatography with silica gel (CH_2Cl_2, R_f = 0.6), followed by recrystallization from chloroform to afford **7** (94 mg, 16%) as a red solid. **7**: mp 235.0−236.0 °C; ^{1}H NMR (600 MHz, $CDCl_3$) δ 6.43 (s, 2H), 6.79 (s, 1H), 7.51 (dd, J = 8.2, 7.6 Hz, 4H), 7.59 (t, J = 7.6 Hz, 2H), 8.00 (d, J = 8.2 Hz, 4H), 9.04 (s, 1H); ^{13}C NMR (150 MHz, acetone-d_6) δ 94.2, 111.5, 128.2, 129.9, 132.6, 133.7, 149.5, 155.5, 169.9; ^{19}F NMR (565 MHz, $CDCl_3$, ext. $CFCl_3$) δ −140.8 (q, J = 8.6 Hz, 4F); IR (KBr) 3082, 1651, 1555, 1512, 1489, 1397, 1192, 1053 cm^{-1}; EIMS (m/z) (rel intensity) 412 (M^+; 100), 411 (92), 105 (36). Anal. Calcd for $C_{20}H_{14}B_2F_4N_2O_2$: C, 58.31; H, 3.43; N, 6.80. Found: C, 58.29; H, 3.23; N, 6.59.

■ ASSOCIATED CONTENT

Supporting Information

^{1}H and ^{13}C NMR spectra, DFT calculation data, X-ray crystal structures, UV−vis absorption and fluorescence spectra and tables of properties are included. This material is available free of charge via the Internet at http://pubs.acs.org.

■ AUTHOR INFORMATION

Corresponding Author

*E-mail: kubota@gifu-u.ac.jp; matsuim@gifu-u.ac.jp.

Notes

The authors declare no competing financial interest.

■ ACKNOWLEDGMENTS

This work was supported by JSPS KAKENHI (23750228, Grant-in-Aid for Young Scientists (B)) and JST A-STEP (AS242Z02734M).

■ REFERENCES

(1) (a) Loudet, A.; Burgess, K. *Chem. Rev.* **2007**, *107*, 4891. (b) Ulrich, G.; Ziessel, R.; Harriman, A. *Angew. Chem., Int. Ed.* **2008**, *47*, 1184. (c) Benstead, M.; Mehl, G. H.; Boyle, R. W. *Tetrahedron* **2011**, *67*, 3573.

(2) (a) Douglass, J. E.; Barelski, P. M.; Blankenship, R. M. *J. Heterocycl. Chem.* **1973**, *10*, 255. (b) Kubota, Y.; Tsuzuki, T.; Funabiki, K.; Ebihara, M.; Matsui, M. *Org. Lett.* **2010**, *12*, 4010.

(3) (a) Nagai, A.; Kokado, K.; Nagata, Y.; Arita, M.; Chujo, Y. *J. Org. Chem.* **2008**, *73*, 8605. (b) Maeda, H.; Mihashi, Y.; Haketa, Y. *Org. Lett.* **2008**, *10*, 3179. (c) Ono, K.; Yoshikawa, K.; Tsuji, Y.; Yamaguchi, H.; Uozumi, R.; Tomura, M.; Taga, K.; Saito, K. *Tetrahedron* **2007**, *63*, 9354. (d) Zhang, G.; Lu, J.; Sabat, M.; Fraser, C. L. *J. Am. Chem. Soc.* **2010**, *132*, 2160.

(4) Kubota, Y.; Hara, H.; Tanaka, S.; Funabiki, K.; Matsui, M. *Org. Lett.* **2011**, *13*, 6544. (b) Kubota, Y.; Tanaka, S.; Funabiki, K.; Matsui, M. *Org. Lett.* **2012**, *14*, 4682.

(5) Yoshino, J.; Furuta, A.; Kambe, T.; Itoi, H.; Kano, N.; Kawashima, T.; Ito, Y.; Asashima, M. *Chem.—Eur. J.* **2010**, *16*, 5026. (b) Yoshino, J.; Kano, N.; Kawashima, T. *Chem. Commun.* **2007**, 559.

(6) Kobayashi, H.; Ogawa, M.; Alford, R.; Choyke, P. L.; Urano, Y. *Chem. Rev.* **2010**, *110*, 2620. (b) Shao, J.; Sun, H.; Guo, H.; Ji, S.; Zhao, J.; Wu, W.; Yuan, X.; Zhang, C.; James, T. D. *Chem. Sci.* **2012**, *3*, 1049.

(7) Lovell, J. F.; Liu, T. W. B.; Chen, J.; Zheng, G. *Chem. Rev.* **2010**, *110*, 2839. (b) Ozlem, S.; Akkaya, E. U. *J. Am. Chem. Soc.* **2009**, *131*, 48. (c) Wang, J.; Hou, Y.; Lei, W.; Zhou, Q.; Li, C.; Zhang, B.; Wang, X. *ChemPhysChem* **2012**, *13*, 2739.

(8) Gómez-Durán, C. F. A.; García-Moreno, I.; Costela, A.; Martin, V.; Sastre, R.; Bañuelos, J.; López Arbeloa, F.; López Arbeloa, I.; Peña-Cabrera, E. *Chem. Commun.* **2010**, 5103. (b) Sisk, W. N.; Ono, N.; Yano, T.; Wada, M. *Dyes Pigm.* **2002**, *55*, 143.

(9) Ertan-Ela, S.; Yilmaz, M. D.; Icli, B.; Dede, Y.; Icli, S.; Akkaya, E. U. *Org. Lett.* **2008**, *10*, 3299. (b) Rousseau, T.; Cravino, A.; Bura, T.; Ulrich, G.; Ziessel, R.; Roncali, J. *Chem. Commun.* **2009**, 1673. (c) Mao, M.; Wang, J.-B.; Xiao, Z.-F.; Dai, S.-Y.; Song, Q.-H. *Dyes Pigm.* **2012**, *94*, 224.

(10) Zhang, D.; Wen, Y.; Xiao, Y.; Yu, G.; Liu, Y.; Qian, X. *Chem. Commun.* **2008**, 4777. (b) Kubota, Y.; Uehara, J.; Funabiki, K.; Matsui, M. *Tetrahedron. Lett.* **2010**, *51*, 6195.

(11) Umezawa, K.; Nakamura, Y.; Makino, H.; Citterio, D.; Suzuki, K. *J. Am. Chem. Soc.* **2008**, *130*, 1550. (b) Nepomnyashchii, A. B.; Bröring, M.; Ahrens, J.; Bard, A. J. *J. Am. Chem. Soc.* **2011**, *133*, 8633. (c) Gresser, R.; Hartmann, H.; Wrackmeyer, M.; Leo, K.; Riede, M. *Tetrahedron* **2011**, *67*, 7148. (d) Kowada, T.; Yamaguchi, S.; Ohe, K. *Org. Lett.* **2010**, *12*, 296. (e) Bura, T.; Retailleau, P.; Ulrich, G.; Ziessel, R. *J. Org. Chem.* **2011**, *76*, 1109. (f) Chen, J.; Burghart, A.; Derecskei-Kovacs, A.; Burgess, K. *J. Org. Chem.* **2000**, *65*, 2900. (g) Goze, C.; Ulrich, G.; Mallon, L. J.; Allen, B. D.; Harriman, A.; Ziessel, R. *J. Am. Chem. Soc.* **2006**, *128*, 10231.

(12) Araneda, J. F.; Piers, W. E.; Heyne, B.; Parvez, M.; McDonald, R. *Angew. Chem., Int. Ed.* **2011**, *50*, 12214. (b) Li, Y.; Patrick, B. O.; Dolphin, D. *J. Org. Chem.* **2009**, *74*, 5237. (c) Li, W.; Lin, W.; Wang, J.; Guan, X. *Org. Lett.* **2013**, *15*, 1768. (d) Bañuelos, J.; López Arbeloa, F.; Martinez, V.; Liras, M.; Costela, A.; García Moreno, I.; López Arbeloa, I. *Phys. Chem. Chem. Phys.* **2011**, *13*, 3437. (e) Zhou, Y.; Xiao, Y.; Li, D.; Fu, M.; Qian, X. *J. Org. Chem.* **2008**, *73*, 1571. (f) Hachiya, S.; Inagaki, T.; Hashizume, D.; Maki, S.; Niwa, H.; Hirano, T. *Tetrahedron. Lett.* **2010**, *51*, 1613. (g) Mao, M.; Xiao, S.; Yi, T.; Zou, K. *J. Fluorine Chem.* **2011**, *132*, 612. (h) Wu, L.; Burgess, K. *J. Am. Chem. Soc.* **2008**, *130*, 4089. (i) Yan, W.; Wan, X.; Chen, Y. *J. Mol. Struct.* **2010**, *968*, 85. (j) Xia, M.; Wu, B.; Xiang, G. *J. Fluorine Chem.* **2008**, *129*, 402. (k) Kobayashi, N.; Takeuchi, Y.; Matsuda, A. *Angew. Chem., Int. Ed.* **2007**, *46*, 758. (l) Singh, R. S.; Yadav, M.; Gupta, R. K.; Pandey, R.Pandey, D. S. *Dalton Trans.* **2013**, *42*, 1696.

(13) Fischer, G. M.; Daltrozzo, E.; Zumbusch, A. *Angew. Chem., Int. Ed.* **2011**, *50*, 1406. (b) Curiel, D.; Más-Montoya, M.; Usea, L.; Espinosa, A.; Orenes, R. A.; Molina, P. *Org. Lett.* **2012**, *14*, 3360. (c) Traven, V. F.; Chibisova, T. A.; Manaev, A. V. *Dyes Pigm.* **2003**, *58*, 41. (d) Guliyev, R.; Ozturk, S.; Sahin, E.; Akkaya, E. U. *Org. Lett.* **2012**, *14*, 1528.

(14) Fischer, G. M.; Ehlers, A. P.; Zumbusch, A.; Daltrozzo, E. *Angew. Chem., Int. Ed.* **2007**, *46*, 3750. (b) Hayashi, Y.; Yamaguchi, S.; Cha, W. Y.; Kim, D.; Shinokubo, H. *Org. Lett.* **2011**, *13*, 2992. (c) Fischer, G. M.; Isomäki-Krondahl, M.; Göttker-Schnetmann, I.; Daltrozzo, E.; Zumbusch, A. *Chem.—Eur. J.* **2009**, *15*, 4857. (d) Feng, J.; Liang, B.; Wang, D.; Xue, L.; Li, X. *Org. Lett.* **2008**, *10*, 4437.

(15) Fischer, G. M.; Jüngst, C.; Isomäki-Krondahl, M.; Gauss, D.; Möller, H. M.; Daltrozzo, E.; Zumbusch, A. *Chem. Commun.* **2010**, 5289.

(16) Berezin, M. Y.; Akers, W. J.; Guo, K.; Fischer, G. M.; Daltrozzo, E.; Zumbusch, A.; Achilefu, S. *Biophys. J.* **2009**, *97*, 22.

(17) Li, H.-J.; Fu, W.-F.; Li, L.; Gan, X.; Mu, W.-H.; Chen, W.-Q.; Duan, X.-M.; Song, H.-B. *Org. Lett.* **2010**, *12*, 2924.

(18) Matichak, J. D.; Hales, J. M.; Barlow, S.; Perry, J. W.; Marder, S. R. *J. Phys. Chem. A* **2011**, *115*, 2160. (b) Matichak, J. D.; Hales, J. M.; Ohira, S.; Barlow, S.; Jang, S.-H.; Jen, A. K.-Y.; Brédas, J.-L.; Perry, J. W.; Marder, S. R. *ChemPhysChem* **2010**, *11*, 130.

(19) Zhou, Y.; Kim, J. W.; Nandhakumar, R.; Kim, M. J.; Cho, E.; Kim, Y. S.; Jang, Y. H.; Lee, C.; Han, S.; Kim, K. M.; Jang-Joo Kim, J.-J.; Yoon, J. *Chem. Commun.* **2010**, 6512. (b) Wang, D. L. K.; Huang, S.; Qu, S.; Liu, X.; Zhu, Q.; Zhang, H.; Wang, Y. J. *Mater. Chem.* **2011**, *21*, 15298. (c) Li, D.; Yuan, Y.; Bi, H.; Yao, D.; Zhao, X.; Tian, W.; Wang, Y.; Zhang, H. *Inorg. Chem.* **2011**, *50*, 4825.

(20) Ito, F.; Nagai, T.; Ono, Y.; Yamaguchi, K.; Furuta, H.; Nagamura, T. *Chem. Phys. Lett.* **2007**, *435*, 283. (b) Qin, W.; Rohand, T.; Baruah, M.; Stefan, A.; Van der Auweraer, M.; Dehaen, W.; Boens, N. *Chem. Phys. Lett.* **2006**, *420*, 562.

(21) Frisch, M. J.; Trucks, G. W.; Schlegel, H. B.; Scuseria, G. E.; Robb, M. A.; Cheeseman, J. R.; Montgomery, J. A., Jr.; Vreven, T.; Kudin, K. N.; Burant, J. C.; Millam, J. M.; Iyengar, S. S.; Tomasi, J.; Barone, V.; Mennucci, B.; Cossi, M.; Scalmani, G.; Rega, N.; Petersson, G. A.; Nakatsuji, H.; Hada, M.; Ehara, M.; Toyota, K.;

Fukuda, R.; Hasegawa, J.; Ishida, M.; Nakajima, T.; Honda, Y.; Kitao, O.; Nakai, H.; Klene, M.; Li, X.; Knox, J. E.; Hratchian, H. P.; Cross, J. B.; Adamo, C.; Jaramillo, J.; Gomperts, R.; Stratmann, R. E.; Yazyev, O.; Austin, A. J.; Cammi, R.; Pomelli, C.; Ochterski, J. W.; Ayala, P. Y.; Morokuma, K.; Voth, G. A.; Salvador, P.; Dannenberg, J. J.; Zakrzewski, V. G.; Dapprich, S.; Daniels, A. D.; Strain, M. C.; Farkas, O.; Malick, D. K.; Rabuck, A. D.; Raghavachari, K.; Foresman, J. B.; Ortiz, J. V.; Cui, Q.; Baboul, A. G.; Clifford, S.; Cioslowski, J.; Stefanov, B. B.; Liu, G.; Liashenko, A.; Piskorz, P.; Komaromi, I.; Martin, R. L.; Fox, D. J.; Keith, T.; Al-Laham, M. A.; Peng, C. Y.; Nanayakkara, A.; Challacombe, M.; Gill, P. M. W.; Johnson, B.; Chen, W.; Wong, M. W.; Gonzalez, C.; Pople, J. A. *Gaussian 09*, Revision A.02; Gaussian, Inc.: Wallingford, CT, 2009.

(22) Hong, Y.; Lam, J. W. Y.; Tang, B. Z. *Chem. Commun.* **2009**, 4332. (b) Hong, Y.; Lam, J. W. Y.; Tang, B. Z. *Chem. Soc. Rev.* **2011**, *40*, 5361.

(23) Caldwell, R. A.; Jacobs, L. D.; Furlani, T. R.; Nalley, E. A.; Laboy, J. *J. Am. Chem. Soc.* **1992**, *114*, 1623. (b) Gorman, A.; Killoran, J.; O'Shea, C.; Kenna, T.; Gallagher, W. M.; O'Shea, D. F. *J. Am. Chem. Soc.* **2004**, *126*, 10619.

(24) Mataga, N.; Kaifu, Y.; Koizumi, M. *Bull. Chem. Soc. Jpn.* **1956**, *29*, 465. (b) Lippert, V. E. *Z. Elektrochem.* **1957**, *61*, 962.

(25) Hu, R.; Lager, E.; Aguilar-Aguilar, A.; Liu, J.; Lam, J. W. Y.; Sung, H. H. Y.; Williams, I. D.; Zhong, Y.; Wong, K. S.; Peña-Cabrera, E.; Tang, B. Z. *J. Phys. Chem. C* **2009**, *113*, 15845. (b) Moyon, N. S.; Mitra, S. *J. Phys. Chem. A.* **2011**, *115*, 2456.

(26) Grabowski, Z. R.; Rotkiewicz, K.; Rettig, W. *Chem. Rev.* **2003**, *103*, 3899. (b) Kokado, K.; Chujo, Y. *J. Org. Chem.* **2011**, *76*, 316. (c) Thomas, K. R. J.; Kapoor, N.; Bolisetty, M. N. K. P.; Jou, J.-H.; Chen, Y.-L.; Jou, Y.-C. *J. Org. Chem.* **2012**, *77*, 3921.

(27) Park, S.-Y.; Ebihara, M.; Kubota, Y.; Funabiki, K.; Matsui, M. *Dyes Pigm.* **2009**, *82*, 258. (b) Ooyama, Y.; Okamoto, T.; Yamaguchi, T.; Suzuki, T.; Hayashi, A.; Yoshida, K. *Chem.—Eur. J.* **2006**, *12*, 7827. (c) Shirai, K.; Matsuoka, M.; Fukunishi, K. *Dyes Pigm.* **1999**, *42*, 95.